Biomedicine & Pharmacotherapy 155 (2022) 113267

Contents lists available at ScienceDirect

Biomedicine & Pharmacotherapy

journal homepage: www.elsevier.com/locate/biopha

Anti-inflammatory and anti-oxidant properties of *Ipomoea nil* (Linn.) Roth significantly alleviates cigarette smoke (CS)-induced acute lung injury via possibly inhibiting the NF-κB pathway

Ling-Hui Zeng [a], Mobeen Fatima [b], Shahzada Khurram Syed [c], Saira Shaukat [b], Amina Mahdy [d], Nadia Hussain [e], Amal H.I. Al Haddad [f], Amira S.A. Said [g,h,i], Ali Alqahtani [j], Taha Alqahtani [j], Abdul Majeed [k], Muhammad Tariq [b], Musaddique Hussain [b,*]

[a] *Department of Pharmacology, Zhejiang University City College, 51 Huzhou Street, Hangzhou 310015, China*
[b] *Department of Pharmacology, Faculty of Pharmacy, The Islamia University of Bahawalpur, Bahawalpur 63100, Pakistan*
[c] *School of Health Sciences, University of Management and Technology Lahore, Pakistan*
[d] *Medical Pharmacology Department, International School of Medicine, Istanbul Medipol University, Istanbul, Turkey*
[e] *Department of Pharmaceutical Sciences, College of Pharmacy, Al Ain University, Al Ain 64141, United Arab Emirates*
[f] *Chief Operations Office, Sheikh Shakbout Medical City (SSMC), Abu Dhabi, UAE*
[g] *Department of Clinical Pharmacy, College of Pharmacy, Al Ain University, Abu Dhabi, United Arab Emirates*
[h] *AAU Health and Biomedical Research Center, Al Ain University, Abu Dhabi, United Arab Emirates*
[i] *Clinical Pharmacy Department, Faculty of Pharmacy, Beni-Suef University, Beni-Suef, Egypt*
[j] *Department of Pharmacology, College of Pharmacy, King Khalid University, Abha 62529, Saudi Arabia*
[k] *Faculty of Pharmacy, Bahauddin Zakariya University, Multan 60000, Pakistan*

ARTICLE INFO

Keywords:
Acute lung injury
Oxidative stress
Pro-inflammatory cytokines
RAW 264.7 macrophage
Lipoxygenase pathway
NF-κB p65

ABSTRACT

Acute respiratory distress syndrome (ARDS), a serious manifestation of acute lung injury (ALI), is a debilitating inflammatory lung disease that is caused by multiple risk factors. One of the primary causes that can lead to ALI/ARDS is cigarette smoke (CS) and its primary mode of action is via oxidative stress. Despite extensive research, no appropriate therapy is currently available to treat ALI/ARDS, which means there is a dire need for new potential approaches. In our study we explored the protective effects of 70 % methanolic-aqueous extract of *Ipomoea nil* (Linn.) Roth, named as In.Mcx against CS-induced ALI mice models and RAW 264.7 macrophages because *Ipomoea nil* has traditionally been used to treat breathing irregularities. Male Swiss albino mice (20–25 ± 2 g) were subjected to CS for 10 uninterrupted days in order to establish CS-induced ALI murine models. Dexamethasone (1 mg/kg), In.Mcx (100 200, and 300 mg/kg) and normal saline (10 mL/kg) were given to respective animal groups, 1 h before CS-exposure. 24 h after the last CS exposure, the lungs and bronchoalveolar lavage fluid (BALF) of all euthanized mice were harvested. Altered alveolar integrity and elevated lung weight-coefficient, total inflammatory cells, oxidative stress, expression of pro-inflammatory cytokines (IL-1β and IL-6) and chemokines (KC) were significantly decreased by In.Mcx in CS-exposed mice. In.Mcx also revealed significant lowering IL-1β, IL-6 and KC expression in CSE (4 %)-activated RAW 264.7 macrophage. Additionally, In.Mcx showed marked enzyme inhibition activity against Acetylcholinesterase, Butyrylcholinesterase and Lipoxygenase. Importantly, In.Mcx dose-dependently and remarkably suppressed the CS-induced oxidative stress via not only reducing the MPO, TOS and MDA content but also improving TAC production in the lungs. Accordingly, HPLC analysis revealed the presence of many important antioxidant components. Finally, In.Mcx showed a marked decrease in the NF-κB expression both in in vivo and in vitro models. Our findings suggest that In.Mcx has positive therapeutic effects against CS-induced ALI via suppressing uncontrolled inflammatory response, oxidative stress, lipoxygenase and NF-κB p65 pathway.

* Corresponding author.
E-mail address: musaddique.hussain@iub.edu.pk (M. Hussain).

https://doi.org/10.1016/j.biopha.2022.113267
Received 7 March 2022; Received in revised form 13 May 2022; Accepted 6 June 2022
Available online 30 September 2022

1. Introduction

Acute respiratory distress syndrome (ARDS) is a collection of pathophysiologic aberrations of the lungs and is initiated by various inciting factors. ARDS is manifested by increased alveolar-capillary membrane permeability, neutrophil aggregation, compromised surfactant formation and edema that leads to reduced respiratory compliance and life-threatening hypoxemia [1]. ARDS complications include pulmonary hypertension, intravascular coagulation, cognitive problems, muscle weakness [2], and cardiovascular diseases [3]. The mortality rate is high (26–61.5 %) [4] and no specific therapeutic agents exist to treat this disorder effectively.

One of the major risk factors in the development of ARDS remains cigarette smoke (CS). Free radicals including alkyl, nitric oxide, peroxyl, semi-quinone, superoxide anion, and several others are present in CS. CS exposure leads to oxidative alteration of the lung's structural components because of the presence of its free radicals or direct activation of macrophages. Activated macrophages stimulate neutrophils and produce cytokines such as interleukins (IL-1β, IL-6 and IL-8) and tumor necrosis factor-α (TNF-α) that are transcribed by NF-κB [5]. Neutrophils release toxic mediators and reactive oxygen species. Subsequently, the equilibrium between oxidants (either endogenous or exogenous) and lungs' antioxidants is altered [6] which results in increased pulmonary and endothelial permeability [7], encouraging infiltration of inflammatory cells.

The lipoxygenase enzyme (LOX), which is expressed in macrophages, neutrophils, and bronchial epithelial cells, produces proinflammatory leukotrienes (LTs) from free arachidonic acid (AA) in collaboration with the 5-lipoxygenase activating protein (FLAP). 5-LOX enzymes are known to have a role in the pathogenesis of various diseases and allergic responses by stimulating the proinflammatory cascade [8]. Leukotriene B_4 (LTB_4) is chemotactic for neutrophils and also promotes IL-6 expression by upregulating its gene transcription [9]. The exaggerated inflammatory response leads to acute lung injury, poor lung compliance, and hypoxemia [10].

Nuclear factor-kappa B (NF-κB), a heterodimer consisting largely of P50 and P65, is a redox-sensitive inflammatory transcription factor. In unstimulated cells, NF-κB remains inactive in the cytoplasm due to the activity of an inhibitory protein IκB, particularly IκBα [11,12]. IκB is quickly phosphorylated by IB kinases (IKK) in response to inflammatory stimuli like CS, and then ubiquitinated and degraded by the proteasome. Subsequently, released NF-κB complex is translocated into the nucleus, where it stimulates the transcription of numerous pro-inflammatory cytokines (TNF-α, IL-1β, IL-6, IL-8) and other inflammatory mediators (PGD_2/E_2 and nitric oxide), which may have a role in CS-induced airway inflammation [13,14]. NF-κB signaling is influenced by oxidative stress and inflammatory cytokines, both of which are present in or produced by tobacco smoke. Evidence has revealed that inhibiting NF-κB not only reduced the oxidative stress and production of pro-inflammatory cytokine but also reduced pulmonary oedema and neutrophil influx, both of which are hallmarks of ALI [15,16].

Recovery from ALI requires proper inflammatory regulation. The cholinergic anti-inflammatory pathway (CAP) dampens the oxidative stress and inflammation [17,18]. Acetylcholine (ACh), produced in response to vagus nerve stimulation, restrict the expression of proinflammatory cytokines [19,20] by inhibiting NF-κB and Janus kinase (JAK-2) / signal transducer activator of transcription (STAT-3) / suppressor of cytokine signaling (SOCS-3) pathway [21]. Cholinesterases (ChEs) are carboxylesterase family of enzymes and cleave ACh into choline and acetic acid and decreasing its concentration in the synaptic cleft. There are two important types of ChEs; acetylcholinesterase (AChE) and butyrylcholinesterase (BChE) /pseudocholinesterase and these are widely expressed in all tissues. The inhibition of AChE and BuChE improves cholinergic function and reduces pulmonary inflammation [22].

Over the millennia, there have been several instances of humans using indigenous plants as an alternative therapeutic option for reasons such as cost, lower adverse effects and other therapeutic constraints of conventional medicines. *Ipomoea nil* (Linn) Roth (Convolvulaceae) locally known as morning glory is found in residential home gardens, meadows, and along the sides of roads [23]. The seeds of *Ipomoea nil* are known as *kala'danah* or *Takhum-e-Nilopaich*. Various phytochemicals including; polyphenols, alkaloids, flavonoids, mucilage, saponins, tannins, terpenoids and psychoactive agents such as chanoclavine, elymoclavine, isopenniclavine, lysergol and penniclavine have been identified in the seeds of *Ipomoea nil* [23]. Theseare traditionally used to treat edema, bronchitis, gastroenteritis, cephalalgiaand skin diseases [24]. Several pharmacological activities particularly, antifungal [25], antioxidant [26,27], anti-inflammatory [28], cytotoxic [29], hepatoprotective [30], antimicrobial [21,24,31,32], anticonvulsant, aphrodisiac [33], antitumor [34,35], anti-nephrotoxic [36], anticancer [37] and antihypertensive activities [38] have been confirmed. However, there are a lack of studies that have focused on its protective effect against CS-induced ALI is missing. In our study, we aimed to examine the protective effect of *Ipomoea nil* (seeds) against ALI using CS-induced ALI murine models and CSE-stimulated RAW 264.7 macrophages cell line.

2. Materials and methods

2.1. Chemicals and kits

All the chemicals utilized in the present research study were of research-grade quality. The chemicals included1,1-diphenyl-2-picrylhydrazyl radical (DPPH), 2,2-azinobis (3-ethylbenzo-thiazoline-6-sulphonicacid)/$ABTS^{+}$,2′,7′-dichlorodihydrofluorescein diacetate (DCFH-DA), acetate buffer, acetonitrile (ACN), dexamethasone, ethanol, ethylenediaminetetraacetic acid (EDTA), formalin (10 %), hematoxylin and eosin (H &E) stain, heparin, methanol, sodium phosphate buffers (Na_2HPO_4), wright-giemsa stain, phosphate buffered saline (PBS) and trolox (analogue of vitamin E) were bought from Sigma Chemical Co. (St. Louis, MO, USA). Ethyl acetate and hydrochloric acid (HCl) were acquired from Merck (Darmstadt, Germany). ELISA kits of IL-6, and IL-1β were obtained from Multi-sciences Biotech Ltd. (Hangzhou, China). Keratinocyte chemoattractant (KC; mouse homolog of IL-8) ELISA kit was procured from 4 A Biotech Co. Ltd. (Beijing, China). ROS and MPO determination kits were purchased from Jiancheng Bioengineering Institute of Nanjing (Nanjing, China). Thermo Fisher Scientific (Waltham, MA, USA) supplied the penicillin/streptomycin antibiotic. RPMI-1640 medium was purchased from GE Healthcare Life Sciences (HyClone Laboratories, Utah, USA).

2.2. Plant material

Kala'danah or dried seeds of Ipomoea nil (2 kg) were purchased from Lahore's historic herbal market, Pakistan. The sample was handed over to the Hortussiccus of Pharmacology research laboratory, Faculty of Pharmacy, The Islamia University of Bahawalpur (IUB), Pakistan, after being certified by an expert botanist as per macroscopic and microscopic peculiarities, and a voucher number was allocated; i.e., IN-SD-08–21–194.

2.3. Extract preparation

Adulterants were initially isolated from seeds by handpicking. Seeds were wiped with a sterile soft cloth to remove dirt or debris before being ground into a coarse powder (#40) using an electronic blender. The coarse powder was macerated in 70 % methanolic solution (MeOH), at ambient temperature for 72 h. The filtration was first made with a sterile muslin cloth to avoid dregs, and then filtered using Whatmann-1 filter paper. The remnant was re-soaked in 70 % MeOH to enhance the extract's yield, and the process was done twice. Filtrates were collected and stored in a jar of amber glass. The extract was concentrated in a

rotary evaporator (Heidolph, Germany) at a speed of 90–120 rpm while maintaining the pressure and temperature (−760 mmHg and 40–45 °C), then preserved at − 4 °C [24].

2.4. HPLC characterization

Acidic hydrolysis of In.Mcx was carried out using the previously published method [39]. In short, the solution comprising In.Mcx (50 mg) and methanol (24 mL) was made, followed by the addition of purified water (16 mL). Then the solution was processed with 6 M HCl (10 mL) and incubated for 2 h at 95 °C. A 0.45 μm nylon filter (Biotech, Germany) was used to filter the mixture before proceeding with the HPLC to avoid impurities. HPLC (SPD-10AV, SHIMADZU, JAPAN) was performed using 250 mm × 4.6 mm, 5 μm, shim-pack CLC-ODS (C-18) column. The gradient HPLC with mobile phase; solvent A (Water: Acetic acid [94:6, at 2.27 pH]), solvent B (acetonitrile [100 %]) was done for phenolic compounds and quercetin. The gradient was set as; 0–15 min (15 % B), 15–30 min (45 % B) and 35–45 min (100 % B) with 1 mL/minute of flow rate. To separate kaempferol, the isocratic HPLC was conducted with a mobile phase acetonitrile: dichloromethane: methanol (60:20:20). A UV/visible HPLC detector was exploited to determine the eluted phenolic components. The retention time and peak areas of isolated components were then matched with the reference standards to identify these components.

2.5. In vitro antioxidant activity (DPPH assay)

The exploration of the free radical scavenging potential of In.Mcx was based on the previously published method with minor modifications [40]. In a 96-well microtitre plate, a 0.1 μM solution having DPPH and methanol was made then incubated for 30 min at 37 °C. Afterwards, a multiplate ELISA reader (Spectra MAX-340, Molecular Devices) was utilized to measure the absorbance (517 nm). Quercetin was used as a reference drug.

2.6. In vitro enzyme inhibitory activity

2.6.1. Acetylcholinesterase (AChE) assay

The colorimetric approach of Ellman was slightly modified to assess AChE inhibition activity [41]. 10 μL AChE was added into the 100 μL solution having 60 μL of 50 mM Na_2HPO_4 buffer and 10 μL of In.Mcx, then incubated at 37 °C for 10 min. The reaction was initiated by adding 10 μL of 0.5 mM acetylthiocholine iodide (substrate) and 10 μL 5, 5′-dithiobis-2-nitrobenzoic acid (DTNB). Subsequently, the solution was incubated for 30 min, and absorbance was measured at 405 nm by a 96-well plate reader (Synergy HT, Biotek, USA). Eserine was employed as a positive control. All tests were done in triplicate along with their controls.

2.6.2. Butyrylcholinesterase (BuChE) assay

The activity of BuChE inhibitory enzyme was determined by a slightly modified form of the Ellman's outlined method [41]. 10 μL of BuChE (Sigma Inc.) was added to the 100 μL solution having pre-mixed 60 μL Na_2HPO_4 buffer and 10 μL of In. Mcx. The solution was pre-read at 405 nm by a 96-well plate reader (Synergy HT, Biotek, USA) and pre-incubated for 10 min at 37 °C. The reaction was catalyzed by adding 10 μL of 0.5 mM butyrylthiocholine iodide 10 μL DTNB, then incubated at 37 °C for a further 30 min and absorbance was taken at 405 nm. All tests were performed in triplicate with corresponding controls, and Eserine was employed as a positive control.

2.6.3. Lipoxygenase (LOXs) assay

The LOXs activity was analyzed by adapting the previously reported method [42]. The 200 μL LOXs assay solution, containing 140 μL Na_2HPO_4 buffers, 20 μL In.Mcx and 15 μL purified LOXs (Sigma Inc.) was pre-incubated (at 25 °C) for 10 min. The reaction was started after adding 25 μL substrate solution, and then absorbance was measured at 234 nm by a 96-well plate reader (Synergy HT, Biotek, USA). This analysis, included both positive (Baicalein) and negative controls, was performed in triplicate.

2.7. Extract solutions

The required amount of In.Mcx was adjusted using an analytical weighing balance, then promptly dissolved in normal saline (NS) to achieve the final concentrations of 100 200, and 300 mg/mL. The standard dose volume was 10 mL/kg; thus, the desired volume was calculated based on body weight for an individual mouse.

2.8. Mice ethicality and handling

Mice were handled ethically for the experimental purposeafter approval from the Animals Research Ethics Committee, Department of Pharmacology, Faculty of Pharmacy, IUB, Pakistan. Six to seven-week-old, healthy Swiss albino male mice (20–25 ± 2 g) were confined in aerated wooden boxes at experimental zone II of the Faculty of Pharmacy, IUB, Pakistan. Mice were kept in thesame warm (24 °C ± 2), humid (40–60 %) conditions, 12 h light/12-hours dark cycle, with free access to water and healthyfood.All of these were attuned before the experiment, and their overall health and body weight were monitored regularly. Six groups of mice were planned, five mice per group, and each group was accurately marked. 1) Control/healthy/ambient air-exposed, 2) CS exposed or model group, 3) Dexa (1 mg/kg), 4) 100 mg/kg of In.Mcx (In.Mcx-1); 5) 200 mg/kg ofIn.Mcx (In.Mcx-2), and 6) 300 mg/kg of In.Mcx (In.Mcx-3).

2.9. CS-induced ALI models

Models of CS-induced ALI were established in line with the previously reported approach [43]. Dexa (1 mg/kg) and In.Mcx (100 200 300 mg/kg) were administered by oral feeding needle to the corresponding groups. One hour after dosing, all groups (besides the healthy controls) were subjected to mainstream CS generated by 3R4F research-grade cigarettes (possessing nearly 29.9 mg nicotine/m^3 and 600 mg TPM/m^3) in a polycarbonate chamber (65 ×50 ×45 cm). Mice were confronted with 10 cigarettes each day (1 cigarette after six minutes). The procedure was repeated for ten consecutive days. All of mice were euthanized by cervical dislocation 24 h following the last CS exposure in order to harvest BALF and lungs.

2.10. Measurement of oxygen saturation

After a 24-hr of the last CS-exposure, oxygen saturation (SO_2) of all the mice was measured by using a moor VMS-OXYTM monitor (Moor Instruments, United Kingdom) that measured the oxygenated/deoxygenated Hb concentration and percentage oxygen saturation in the microcirculation at a wavelength range of 500–650 nm.

2.11. Acquisition of BALF and inflammatory cell counts

After euthanizing all of the mice, the trachea and thoracic cavity were surgically exposed, and the right lungs were ligated to prevent fluid flow. The left lung was infused with pre-cooled sterile NS (0.4 mL) having 1 % FBS and 5000 IU/L heparin. The fluid was then retrieved carefully to prevent shearing force and lavage 3 times [44]. Inflammatory cells were counted in the freshly collected BALF via the Neubauer chamber (Labor Optik, Friedrichsdorf, Germany). The remaining BALF was promptly centrifuged (1000g; 4 °C) for 10 min, and the collected supernatant was maintained at −80 °C for subsequent investigation. To obtain the smears, cell pellets were spread on a microscopic slide. After Wright-Giemsa staining, 200 cells (×10^4/mL BALF) were quantified by two experts [45].

2.12. Albumin assay

Albumin assay of the supernatant of BALF was performed using albumin determination kits at a wavelength of 628 nm. The albumin concentration ratio not only exhibits the effused albumin levels but also indicates the pulmonary microvascular permeability.

2.13. Estimation of the Lung weight coefficient (LWC)

To evaluate the extent of pulmonary edema [46], LWC was estimated. The excised right lungs were aspirated for removal of blood, and then weighed using an analytical weighing scale.

2.14. In vivo assessment of cytokines

The expression of pro-inflammatory cytokines (IL-1β and IL-6) and chemokine (KC) in the preserved supernatant was evaluated using respective ELISA kits in a manner consistent with the manufacturer's guidelines.

2.15. Lung histopathology

The lower lobes of mice's right lungs were fixed in 10 % formalin (neutral) at room temperature and subsequently fixed with paraffin in histology cassettes. Afterward, the fixed lungs were rinsed with water for 2–3 h before being dehydrated with a series of graded alcohols and xylene. Later, the lungs were infiltrated in stainless steel molds stuffed with molten paraffin wax and let it solidifiedon the cold plate, then sectioned (4 μm) by a slicer. Leave the sections dry upright on the charged glass slides to facilitate adhesion, afterward maintained at 60 °C for overnight. Afterward, hematoxylin-eosin (H&E) staining was performed to evaluate the infiltration of neutrophils and inflammatory cells under a Polarized Light Microscope (Olympus BX50). Subsequently, images were captured using an Olympus BX 50 at 20 X and 40 X and the results were processed using Image J software version 1.53 (NIH). Pathologists used the 5-point grading system in order to measure alveolar edema, the severity of the injury, and the presence of inflammatory cells [47]. The extent of lung injury was graded on a scale from 0 (normal) to 5 (severe), and the cumulative mean of all variables was derived. Scoring was performed in a minimum of 3 different fields for an individual lung section and mean scores were derived from the 5 mice.

2.16. Analysis of oxidative stress markers

Since excessive ROS generation generated by CS is a key and direct source of oxidative stress, thus, we also examined the effect of *Ipomoea nil* on ROS levels via ROS assay kit. In brief, lung tissues were snap frozen on dry ice and preserved at − 80 °C before being sliced into small sections then homogenized with lysis solution (5x RIPA buffer) on ice. The homogenized sample was centrifuged at 2000 rpm for 10 min and the harvested supernatant was kept on ice. ROS assay kit was used in accordance with the manufacturers′ instructions to detect the ROS via oxidant-sensitive fluorescent dye (DCFH-DA) method. The data was obtained using a fluorescent plate reader (BioTek, USA) that operated at wavelengths of 484 nm (excitation) and 530 nm (emission). Furthermore, for the testing of MPO contents and MDA activity, the lungs of individual mice were homogenized and centrifuged at 4500g for 10 min and the supernatant was collected to measure the MPO and MDA activity by using the relevantassay kits. All that testing was performed according to the criteria and instructions of the manufacturer. Additionally, respective ELISA kits were used to measure the TAC and TOS contents from BALF. In short, acetate buffer and ABTS (as reagents one and two respectively) were applied for the measurement of TAC. The method developed by Erel [48] was applied and the absorbance was measured by using a semi-auto biochemistry analyzer – Biosystem BTS-330 [49]. While for checking the TOS, the method developed by Erel [50] using o-dianisidine (10 mM), ferrous iron (45 μL in Clark and Lubs solution as reagent 1 and H_2O_2 (7.5 mM) in Clark and Lubs solution as reagent 2. While the spectrophotometric analysis was performed using the same semi-auto biochemistry analyzer (Biosystem BTS-330).

2.17. Preparation of cigarette smoke extract (CSE)

The previously reported methodology was used in preparing the CSE for in vitro analysis [43], whereby PBS (50 mL) was used to filter mainstream smoke from 3R4F research-grade cigarettes over five minutes. After extracting five cigarettes, the CSE was collected. The identical procedure was followed in the formation of the positive control with the exception that there was no cigarette.

2.18. Cell culture and assessment of cell viability

RAW 264.7 macrophage cells, obtained from American Type Culture Collection (ATCC, Manassas, VA, USA), were used to culture mouse leukemic monocyte-macrophage. These cells were grown in RPMI-1640 medium supplemented with 10 % fetal bovine serum (FBS) in the presence of 100 μg/mL streptomycin and 100 U/mL penicillin. The methylthiazol-tetrazolium (MTT) test was performed, as per the manufacturer's specifications, to evaluate the cytotoxicity of In.Mcx (0–100 μM) alone and subsequently combined with CSE (1–10 %). In brief, RAW 264.7 macrophages (4×10^5 cells/mL) were plated for 24 h in 96-well plates. Consequently, treated with In.Mcx (0–100 μM) and incubated at 37 °C for 1 h. Cells were further incubated with CSE (4 %) for 24 h, followed by the addition of MTT (5 mg/mL), and constantly monitored for another 4 h at 37 °C. Eventually, supernatants were substituted with 200 μL/well of DMSO, and optical densities at 570 nm wavelength were determined.

2.19. In vitro cytokines assay via ELISA

To perform an in vitro cytokine assay using ELISA, RAW 264.7 macrophage were seeded to 12-well plates and then culture medium of these plates was replaced with a serum-free RPMI-1640 medium for a duration of 10–12 hrs. After that, RAW 264.7 macrophages were exposed to In.Mcx (10 and 100 μM) for 1 h. After one hour, 12-well plates were exposed to CSE (4 %) for 24 h. After exposure to CSE (4 %), the supernatant was collected and protein levels of IL-1β and IL-6 and KC were measured using ELISA kits according to the manufacturer's protocols.

2.20. Determination of p65-NF-κB by ELISA

ELISA Kit was used (ab176648, abcam) to explore p65-NF-κB. RAW 264.7 macrophages were acclimated to 12-well plates at 70–80 % confluence and then culture medium of these plates was replaced with a serum-free RPMI-1640 medium for a duration of 10–12 h. After that, RAW 264.7 macrophages were exposed to In.Mcx (10 and 100 μM) for 1 h. After one hour, 12-well plates were exposed to CSE (4 %) for 24 h. After treatment, media was removed, followed by washing twice by PBS. Then, the cells were solubilized by using cell extraction buffer and NFκB p65 was measured in these cell lysates using ELISA. Additionally, tissue lysates were typically prepared by homogenization of preserved lungs that is first minced and thoroughly rinsed in PBS to remove blood and centrifuged at 18 000 x g for 20 min at 4 °C to collect supernatants. Absorbance was measured by a plate reader at 450 nm.

2.21. Statistical analysis

The results were presented as means ± standard error mean (SEM). The GraphPad Prism statistical program (version 8.4.2) was used to perform all the analyses and compare *p*-values. One-way ANOVA was performed in order to estimate the *p*-value. $p < 0.05$ (*), $p < 0.01$ (**), p

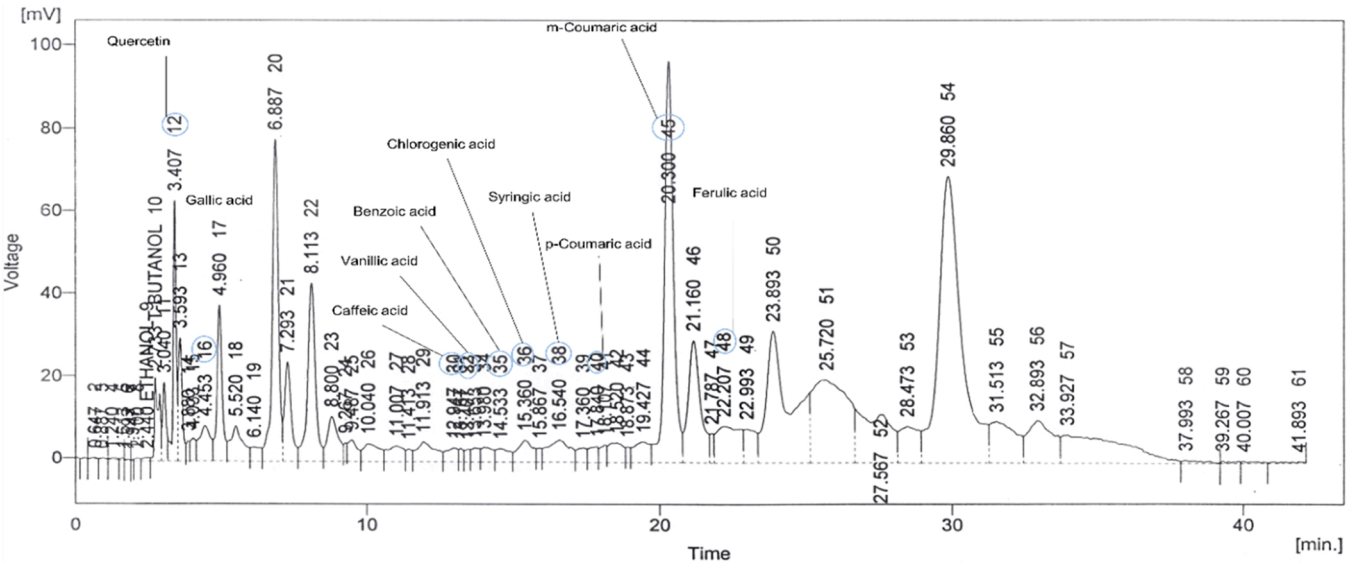

Fig. 1. The HPLC chromatogram of various polyphenols identified in In.Mcx.

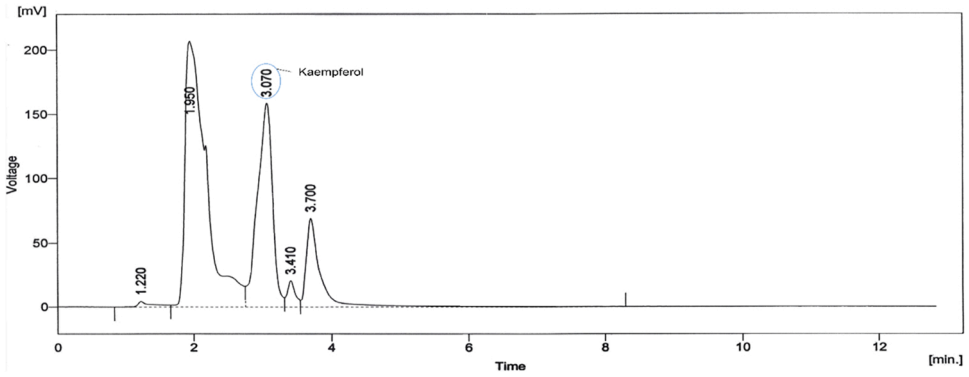

Fig. 2. HPLC chromatogram of kaempferol identified in In.Mcx.

Table 1
List of HPLC-identified compounds in the In.Mcx.

Sr #	RT (min)	Area (mV.s)	Quantity (ppm)	Mol. mass (g/mol)	Possible Compound	Mol. formula
1	14.533	106.659	11.30	122.12	Benzoic acid	$C_6H_5CO_2H$
2	12.947	93.496	4.30	180.16	Caffeic acid	$C_9H_8O_4$
3	186.657	15.360	14.55	354.31	Chlorogenic acid	$C_{16}H_{18}O_9$
4	22.207	509.700	36.69	194.18	Ferulic acid	$C_{10}H_{10}O_4$
5	4.453	220.962	7.95	170.12	Gallic acid	$C_7H_6O_5$
6	3.070	2403.527	961.24	286.23	Kaempferol	$C_{15}H_{10}O_6$
7	20.300	2092.083	25.10	164.16	m-Coumaric acid	$C_9H_8O_3$
8	17.840	85.135	1.10	164.04	p-Coumaric acid	$C_9H_8O_3$
9	3.040	167.334	8.86	302.23	Quercetin	$C_{15}H_{10}O_7$
10	16.540	283.627	7.09	198.17	Syringic acid	$C_9H_{10}O_5$
11	13.167	32.729	2.02	168.14	Vanillic acid	$C_8H_8O_4$

< 0.001 (***) was regarded as significant, highly significant and extremely significant in contrast to the model group respectively whereas $p < 0.05$(#) was considered as significant in comparison to healthy or control group.

3. Results

3.1. HPLC-based characterization of In.Mcx

The HPLC is suitable for both qualitative and quantitative analysis of naturally occurring compounds. Column chromatographic characterization and quantitative modeling were performed on In.Mcx. Flavonoids, including quercetin and kaempferol, along with phenolic acids such syringic acid, ferulic acid, vanillic acid, caffeic acid, coumaric acid, gallic acid and chlorogenic acid were identified in the HPLC analysis. Fig. 1 shows the chromatograms for quercetin and phenolic acidswhile Fig. 2 shows chromatograms for kaempferol. Table 1 lists the quantity of components in ppm.

3.2. In.Mcx's radical scavenging potential

The In.Mcx revealed concentration-dependent free radical

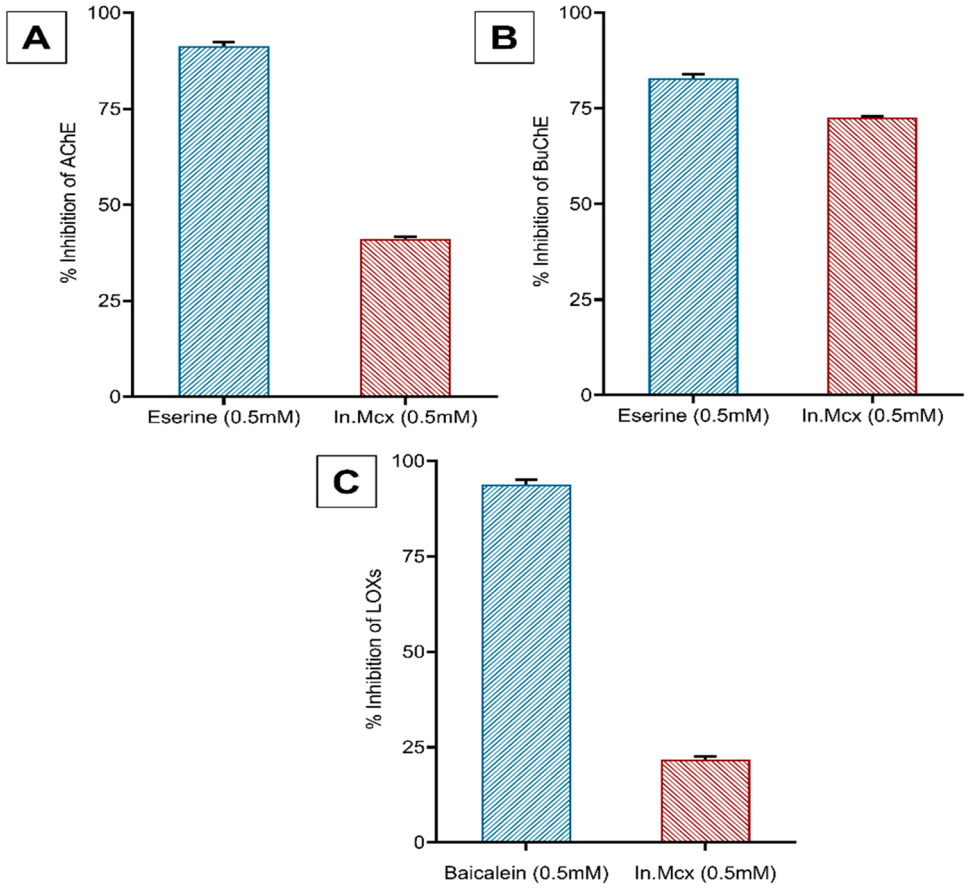

Fig. 3. In.Mcx inhibited AChE, BuChE and LOXs. All the tests were performed in triplicate and results are expressed as mean ± SEM.

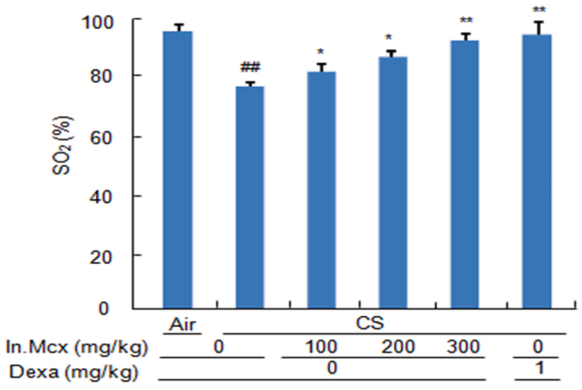

Fig. 4. In.Mcx reduced oxygen saturation (SO_2). SO_2 of all mice was monitored 24 hrs after last CS exposure using the moor VMS-OXYTM monitor (Moor Instruments, United Kingdom). $^{\#\#}p < 0.01$ vs. control group; $^{*}p < 0.05$ and $^{**}p < 0.01$ vs. model group. The results are expressed as the mean ± SEM; n = 5 (each group).

scavenging activity, with the highest inhibition of 88.29 ± 0.15 % reported at 500 μg/mL, comparable to Quercetin that showed 93.21 ± 0.97 % inhibitions of DPPH radicals at 0.3 mM.

3.3. In.Mcx inhibited AChE, BuChE and LOXs

The cholinergic anti-inflammatory pathway (CAP) provides protection from both oxidative stress and inflammation [51]. The percentage AChE inhibitory activity of In.Mcx was 41.16 ± 0.45 with IC_{50} 17.99 ± 0.77 μmol ($p < 0.001$) as compared to 91.29 ± 1.17 with IC_{50} of 0.04 ± 0.01 μmol for of serine (Fig. 3A). While the percentage BuChE inhibition activity of In.Mcx was 72.52 ± 0.39 with IC_{50} 118.02 ± 0.02 μmol ($p < 0.001$) as compared to 82.82 ± 1.09 with IC_{50} of 0.85 + 0.01 μmol with for serine (Fig. 3B). LOXs inhibition reduces inflammation in lung damage [52,53]. The percentage inhibitory response of In.Mcx against LOXs was 21.79 ± 0.74 with IC_{50} 154.21 ± 0.07 μmol ($p < 0.001$) while that of baicalein was 93.79 ± 1.27 with IC_{50} of 22.4 ± 1.3 μmol (Fig. 3C). In.Mcx inhibited lipid peroxidation dose-dependently, confirming its antioxidant action towards lipid peroxidation in CS-induced ALI.

3.4. In.Mcx lowered CS-induced hypoxemia

As expressed in Fig. 4, mice belonging to the CS-groups were presented with hypoxemia (lowered SO_2) while In.Mcx at 300 mg/kg remarkably lowered the CS-induced hypoxemia (elevated SO_2) in a dose-dependent manner ($p < 0.01$).

3.5. In.Mcx suppressed CS-induced pulmonary edema and lung permeability

CS robustly produced oxidative stress by enhancing microvascular permeability and edema, culminating in acute lung injury. Measurement of CS-induced lung permeability and pulmonary edema by measuring the albumin contents and lung weight coefficient respectively revealed a higher albumin contents and lung wet weight coefficient in the CS-treated group than in the fresh air-exposed group ($p < 0.01$). Pretreatment with In.Mcx effectively and dose-dependently decreased the albumin contents ($p < 0.01$) (Fig. 5A) and lung wet weight coefficient ($p < 0.01$) (Fig. 5B).

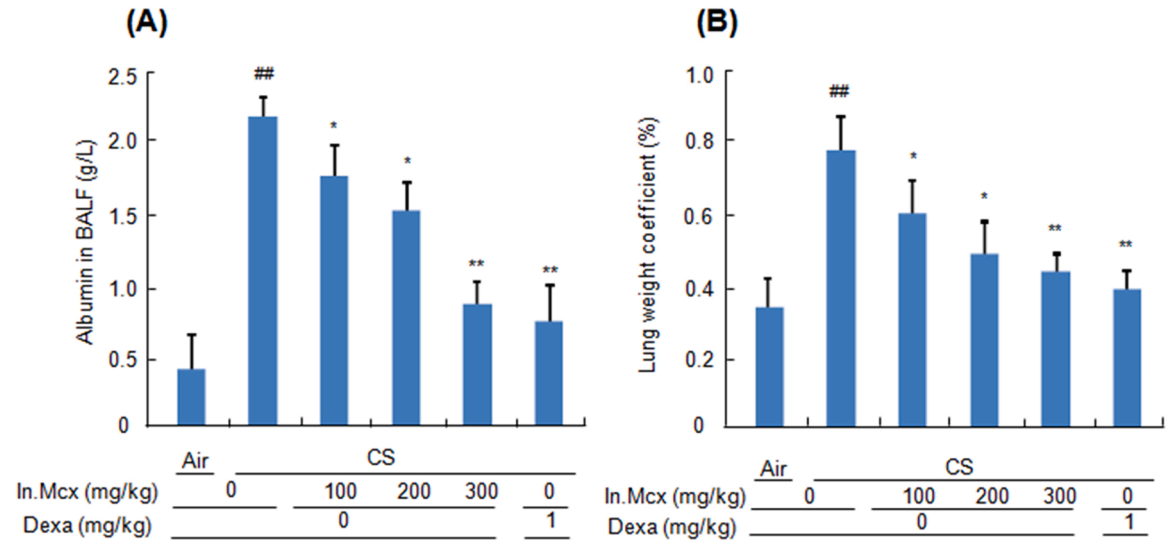

Fig. 5. In.Mcxameliorated the CS-induced lung edema and lung permeability. (A) Using albumin measurement kits, the concentration of albumin in BALF was determined. (B) The lung weight coefficient was calculated by dividing each rat's lung weight by its overall body weight, after the removal of surface blood from dissected lung tissues. $^{\#\#}p < 0.01$ vs. control group; * $p < 0.05$ and * * $p < 0.01$vs. model group. The results are expressed as the mean ± SEM; n = 5 (each group).

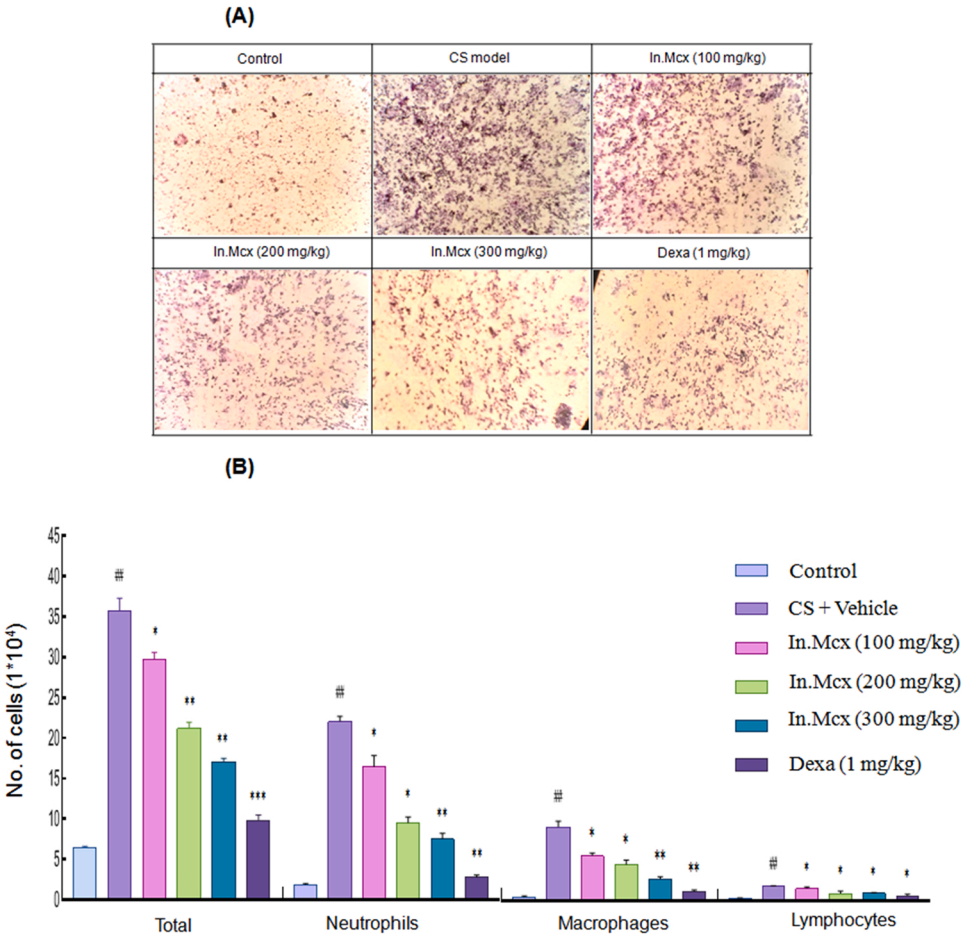

Fig. 6. In.Mcx reduced the inflammatory cells count in BALF collected from the experimental mice. A sufficient volume of BALF was retrieved 24 hrs since the last CS exposure and total number of cells was counted in Neubauer chamber. Pellets obtained after centrifuge from BALF were spread on the slide for overnight, and Wright–Giemsa staining was performed to observe inflammatory cells, neutrophils, macrophage and lymphocytes count under a light microscope based on their morphological criteria. A mature neutrophil has many lobes nucleus (two to five). The nucleus of the monocyte is kidney-shaped. (A) The image of neutrophils, macrophages and lymophocytes in collected BALF. (B) Total cells, macrophages, neutrophils, and lymphocytes infiltration patterns in the BALF. $^{\#\#}p < 0.01$ vs. healthy control group;* $p < 0.05$ and ** $p < 0.01$, *** $p < 0.001$ vs. model group. The results are expressed as the mean ± SEM; n = 5 (each group).

3.6. In.Mcx attenuated CS-elicited inflammatory cell infiltration

Cellular infiltration into the lungs is a major event in the pathogenesis of ALI. Cell counts (mainly neutrophils) increased significantly ($p < 0.01$) after exposure to CS in the CS-exposed group in contrast to the control group. CS inhalation led to a surge of neutrophils in the alveoli, which had been evacuated in the BALF, while pre-treated animals had less neutrophils in their BALF, as shown in Fig. 6A and B. The total number of cells in groups pre-treated with Dexa ($p < 0.001$) and In. Mcx ($p < 0.01$) differed significantly from the CS exposed group. This

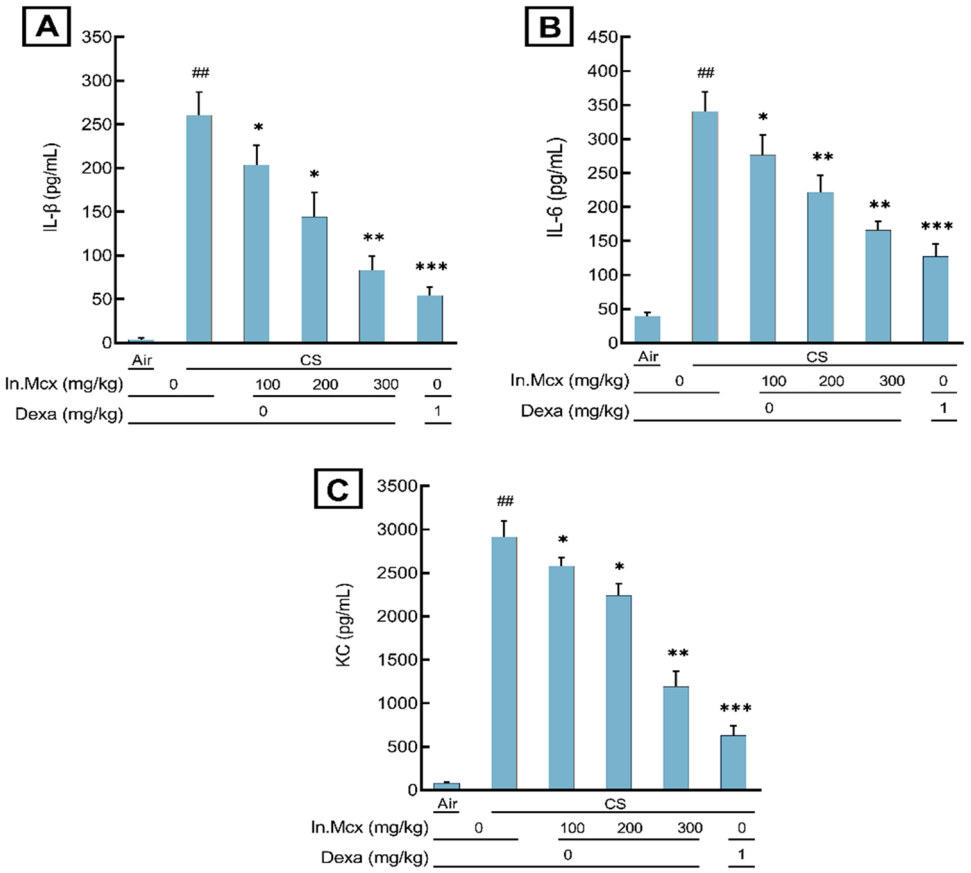

Fig. 7. In.Mcx tapered the CS stimulated expression of pro-inflammatory mediators. ELISA kits were used to evaluate the expression of cytokines. $^{\#\#}p < 0.01$ in comparison to the control group; * $p < 0.05$, ** $p < 0.01$ and *** $p < 0.001$ when compared to the CS exposed group. The values are represented as mean ± SEM; n = 5 (each group).

revealed that In.Mcx might be capable of ameliorating CS-induced ALI.

3.7. In.Mcx impaired CS-induced cytokines expression in vivo

The predominant biomarkers of ALI, such as pro-inflammatory cytokines (especially IL-1β, IL-6) and the chemoattractant (KC), were analyzed with relevant ELISA kits. The expression of IL-1β (Fig. 7A), IL-6 (Fig. 7B), and KC (Fig. 7C) in the model or CS-exposed group was significantly higher ($p < 0.01$) than the control group. Conversely, expression of these markers wasabridged in a dose-dependent manner in the Dexa and In.Mcx groups ($p < 0.01$) relative to model group. These findings suggest that In.Mcx prevented CS-induced ALI against pulmonary damage by suppressing the production of IL-1β, IL-6, and KC.

3.8. In.Mcx ameliorated CS-mediated morphological changes

The effectiveness of In.Mcx in CS-induced ALI was assessed histopathologically via H&E staining of paraffin-embedded lungs. Tissues of fresh air-exposed group demonstrated normal alveolar architecture while the tissues of CS-exposed group revealed peculiar features including increased infiltration of inflammatory cells, neutrophils and macrophages into the alveolar spaces (Fig. 8A). Mice pre-treated with Dexa and In.Mcx had better aeration and less neutrophilsin relation to CS exposed group. The mean pathological index reflected the severity of the damage, inflammatory cell infiltration, and pulmonary edema. The model group had a higher mean pathological score ($p < 0.01$) than the mean of the control group (Fig. 8B) whereas Dexa ($p < 0.001$) and In. Mcx ($p < 0.01$) treated groups had lowered mean pathological scores when compared to CS-exposed mice. Histopathology and mean pathological score indicated that In.Mcx considerably alleviated the severity of ALI.

3.9. In.Mcx mitigated CS-induced oxidative stress

The CS-induced oxidative stress overwhelms the endogenous antioxidants, exacerbating pulmonary damage. The degree of expression of biological markers such as ROS, MPO, MDA,TOS and TAC indicates the presence of oxidative stress in the lung. CS exposure stimulated the generation of ROS, MPO, MDA and TOS while depleting the levels of TAC. Oxidative stress was substantially higher in the CS-exposed groups ($p < 0.01$) than in the control groups as depicted in Fig. 9. However, In. Mcx, in a dose-dependent way attenuated CS-stimulated ROS, MPO, MDA, and TOS and augmented TAC. Pretreatment with Dexa and In.Mcx (300 mg/kg) considerably reduced oxidative stress by not only reducing the ROS (Fig. 9A), MPO activity of lungs (Fig. 9B), MDA (Fig. 9C) and TOS (Fig. 9D) expression but also enhanced TAC (Fig. 9E). A substantial difference ($p < 0.001$) was noticed in both groups (Dexa and In.Mcx) as compared to the model group. These data showed that In.Mcx exhibits antioxidant potential against oxidative stress in CS-induced ALI.

3.10. In.Mcx modulated CS-induced cytokines expression from RAW264.7 macrophages

Based on remarkable in vivo outcomes, we further explored whether antioxidant effect of In.Mcx could prevent the production of cytokines from CSE-stimulated RAW 264.7 macrophages. The MTT assay indicated that exposure of RAW 264.7 macrophages to CSE (4 %) plus In.Mcx up to dosage of 100 μM were not toxic (data not shown).

ELISA was used to assess the effects of In.Mcx on the expression of pro-inflammatory cytokines and chemokines. CSE (4 %) exposure of

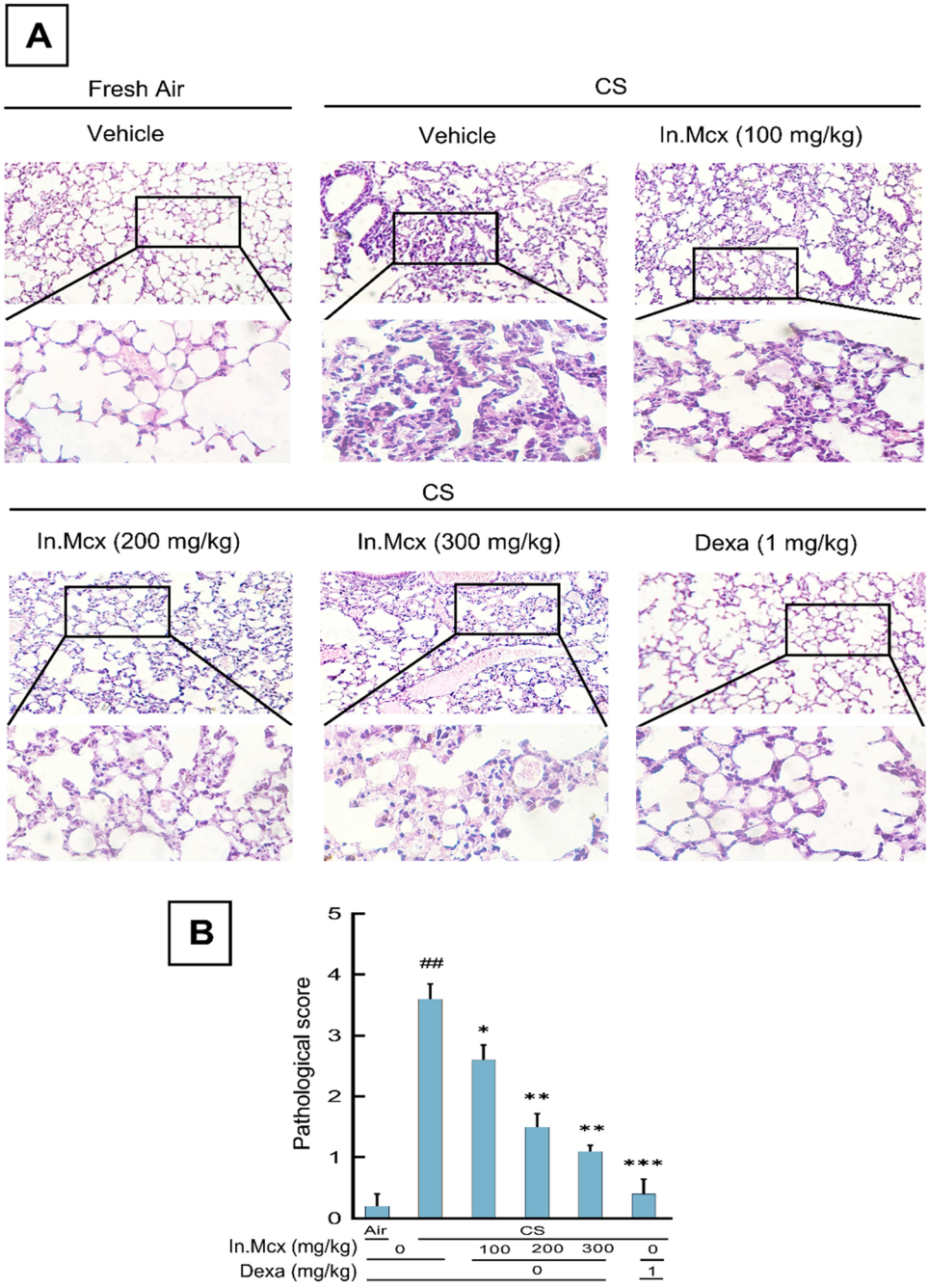

Fig. 8. In.Mcx ameliorated CS-mediated morphological changes and mean pathological score. Lung tissues immersed in paraffin wax subsequently sectioned to a thickness of 4 μm, followed H&E staining. Histopathological assessment was made to validate the invasiveness of neutrophils and inflammatory cells (A), which was also evaluated quantitatively by two expert pathologists (B). Tissues of control (exposed to fresh air) groups are showing the normal architecture of the alveoli while the tissues of the model (CS-exposed group) groups are revealing increased infiltration of neutrophils, macrophages and inflammatory cells into the alveolar spaces. $^{\#\#}p < 0.01$ as opposed to control group; $^{*}p < 0.05$, $^{**}p < 0.01$ and $^{***}p < 0.001$ compared to CS exposed group. The outcomes are stated as the mean ± SEM; n = 5 (each group).

RAW 264.7 macrophages led to dramatically increased expression of IL-1β, IL-6, and KC ($p < 0.001$). Meanwhile pretreated of In.Mcx (10 and 100 μM) drastically decreased ($p < 0.001$) the levels of IL-1β (Fig. 10A), IL-6 (Fig. 10B), and KC (Fig. 10C) produced by CSE-stimulated RAW 264.7 macrophages in a dose dependent pattern. Hence, obtained in vitro results (Fig. 10) were consistent with the in vivo findings (Fig. 7) implying that In.Mcx effectively reduced the production of pro-inflammatory cytokines and chemokines from CSE (4 %)-activated RAW 264.7 macrophages.

3.11. In.Mcx reduced CSE-induced p65-NF-κB activation in vitro and in vivo

ELISA was used to investigate the mechanism by which In.Mcx reduces CS-induced ALI. In this research, effect of In.Mcx on CS-induced NF-κB pathway activation was focused because NF-κB is necessary for the activation of pro-inflammatory mediators, neutrophil infiltration, changes in pulmonary vascular permeability and oxidative stress. As shown in Fig. 11, expression levels of p65-NF-κB were significantly up-regulated in CS-exposed lung tissues and RAW 264.7 macrophages as compared to vehicle treatment. Consequently, In.Mcx treatment at 100 200, and 300 mg/kg in ALI animals and at 10 and 100 μM in RAW 264.7 macrophages dose-dependently decreased CS-induced p65-NF-κB activation ($p < 0.01$) (Fig. 11A and B). Thus, In.Mcx protected against CS-induced ALI by inhibiting the p65-NF-κB signalling pathway.

4. Discussion

ARDS was originally known as “shock lung” almost half a century ago. ARDS leads to severe hypoxemia and respiratory failure due to

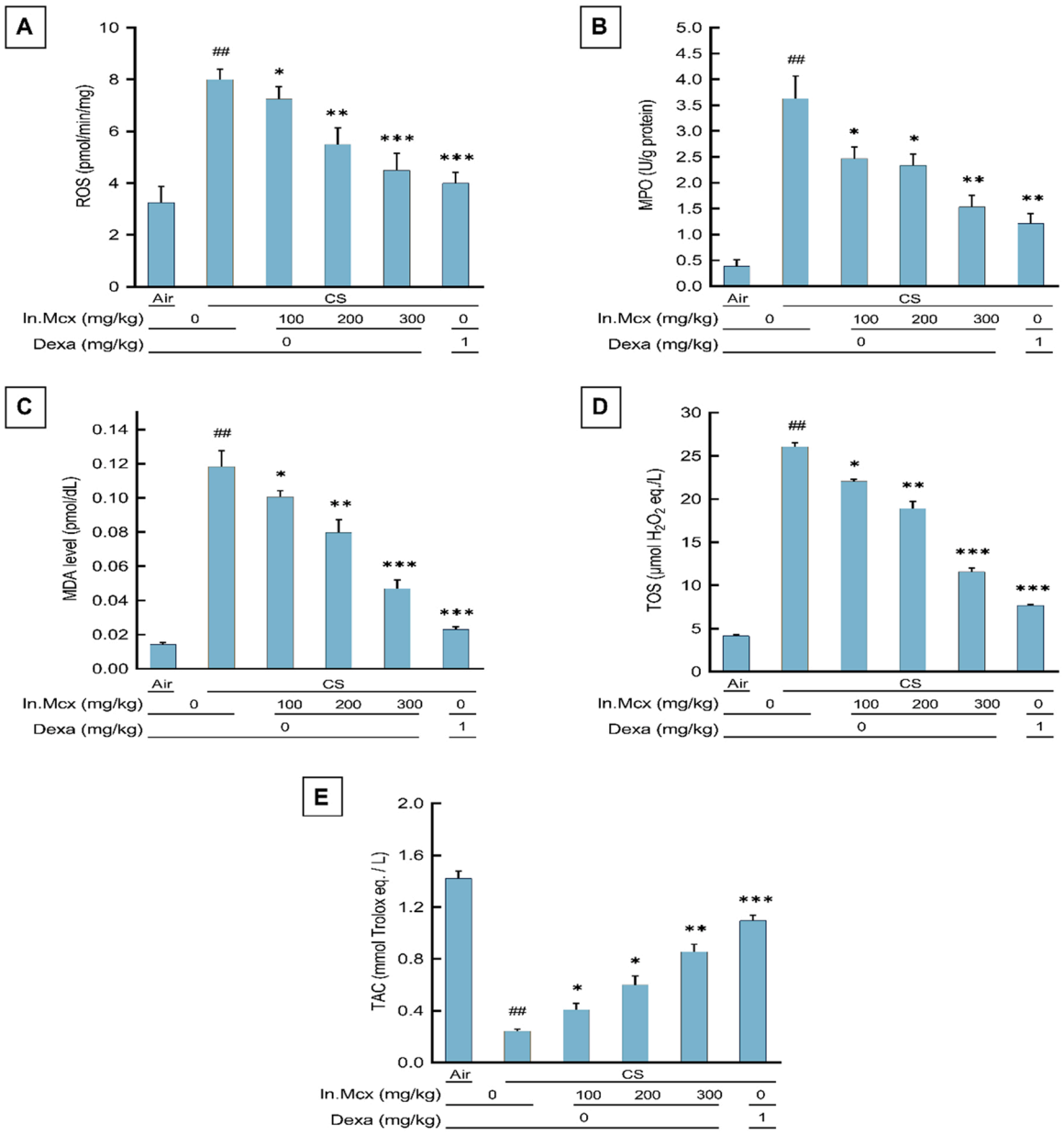

Fig. 9. In.Mcx mitigated CS-induced oxidative stress.The effect of In.Mcx and Dexa on reactive oxygen species (ROS) (A), myeloperoxidase (MPO) (B), malondialdehyde (MDA) (C), total oxidative stress (TOS) (D) and total antioxidant capacity (TAC) (E) was measured by respective ELISA kits and standard curves were determined by xMark™ Microplate Absorbance spectrophotometer. $^{\#\#}p < 0.01$ against control group; * $p < 0.05$, ** $p < 0.01$ and *** $p < 0.001$ versus model group. The findings of these assay are presented as mean ± SEM; n = 5 (each group).

pulmonary edema, inflammatory cell infiltration, and oxidative stress [1]. Many studies have been conducted to understand the pathogenesis of ARDS and explore various treatment strategies but no promising agents have been discovered. This suggests that safe and effective agents are urgently needed against ARDS. *Ipomoea nil* is a potent antioxidant; however, its effect against CS-induced ALI remains undefined and under explored. This research study was designed to assess the impact of *Ipomoea nil* on ameliorating ALI resulting from CS in both in vivo and in vitro models.

Cigarette smoking kills over 3 million people worldwide, even those in developed countries per year. Preclinical and clinical research is increasingly pointing towards CS's detrimental health effects. Smokers, on average, have a 14-year shorter life expectancy than that of non-smokers. CS alone is responsible for higher morbidity and mortality rates than all other combined factors (alcohol intake, accidents, HIV, and illicit drug use). Aside from the direct effect of the toxins (in cigarettes) on the lung, oxidative stress induced by CS perpetuates inflammatory reactions. The mechanisms include 1) Activated macrophages and compromised endothelium (first line of defense) increasing the surface expression of binding molecules and fostering neutrophils' infiltration. 2) Mediating the production of chemokines and pro-inflammatory cytokines, activated macrophages augment the ingress of neutrophils [54]. 3) Having a detrimental effect on neutrophil deformability, stemming their recruitment in the pulmonary microcirculation, a major hallmark of ALI [47].

The antioxidant activity of *Ipomoea nil* has been linked to its various phytochemicals, as shown in various studies [26]. Extensive studies have attempted to investigate the biological properties of polyphenols. Flavonoids (quercetin and kaempferol) are ubiquitously present in fruits, vegetables, and other plants. Flavonoids prevented ALI in mice in many previous studies [55]. Phytochemical study revealed the occurrence of carbohydrates, phenolic substances, glycosides, alkaloids and

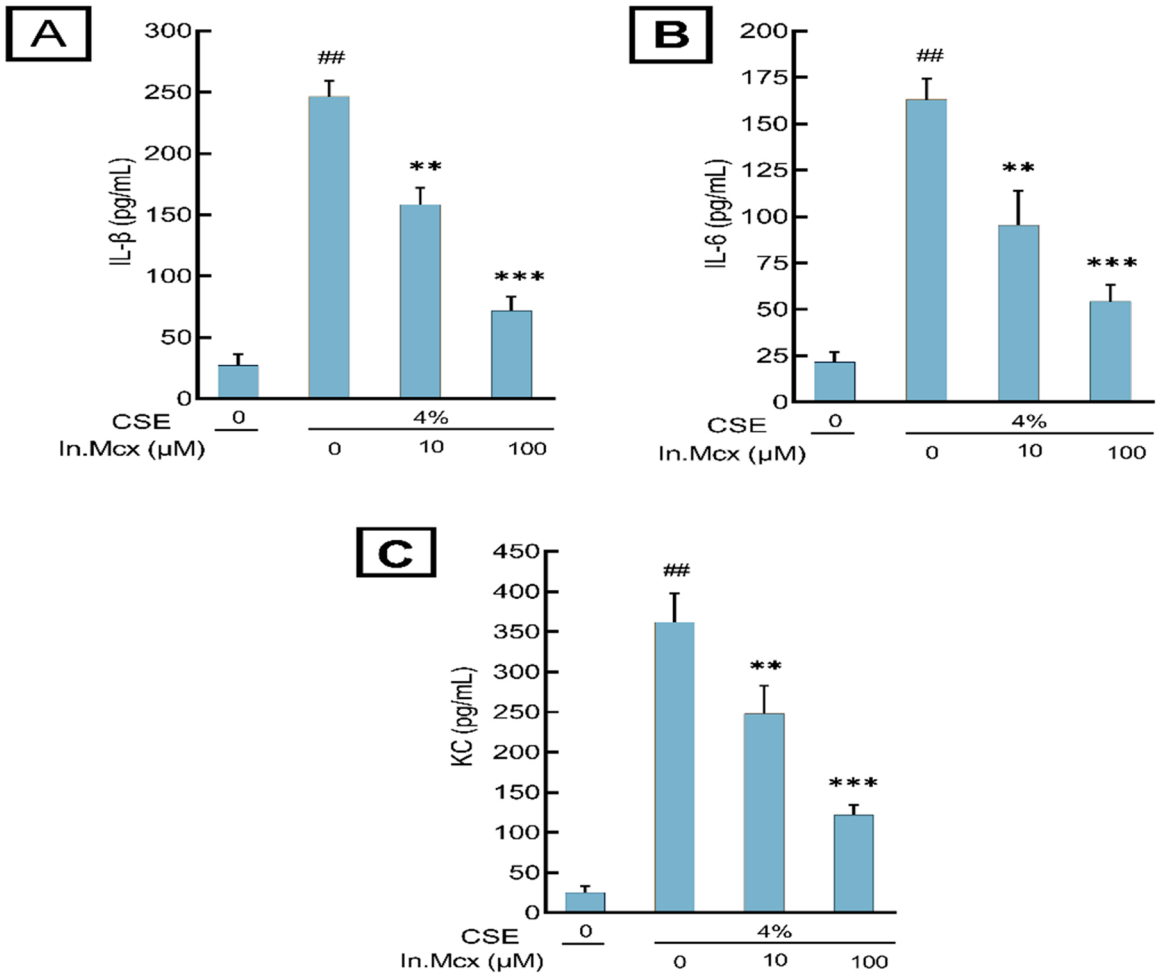

Fig. 10. In.Mcx modulated CS-stimulated cytokines expression from RAW 264.7 macrophages. RAW 264.7 macrophages, pretreated with In.Mcx for 24 hrs, were incubated for 24 hrs with CSE (4 %). The collected supernatant was then subjected to measure the protein expression of IL-1β (A), IL-6 (B) and KC (C) using respective ELISA kits. $^{\#\#}p < 0.01$ versus control group; $^{**}p < 0.01$, and $^{***}p < 0.001$ as opposed to model group. Findings are communicated as mean ± SEM; n = 3 (each group).

tannins [24]. The presence of polyphenols in In.Mcx was also validated by HPLC.

Acetylcholine, also known as Vagusstoff, has an anti-inflammatory effect because it binds to N-shaped acetylcholine receptors (α7nAchR) expressed on neutrophils and macrophages, preventing TNF-α, IL-1β and IL-18 production by inhibiting Nuclear factor-kappaB (NF-κB) and Janus kinase (JAK-2)/signal transducer activator of transcription (STAT-3)/ suppressor of cytokine signaling (SOCS-3) pathways [21]. AChE, a cholinergic synaptic cleft enzyme, catalyzes the conversion of ACh into acetate and choline, restricting its magnitude and duration of the post synaptic potential. AChE has been related to cholinergic activity and neuronal degeneration, as well as regulating proliferation, differentiation, and susceptibility of cells to diverse stimuli such as stress. BuACh also known as pseudocholinesterase is distinguished from AChE by its catalytic preference for butyrylcholine over acetylcholine degradation. It catalyses a greater variety of substrates than AChE. Both (AChE and BuACh) are expressed by the lung's epithelial cells [22]. While increasing the level of ACh, the lung injury could be reduced, as shown in many preclinical studies [51]. In.Mcx significantly antagonized AChE and BuChE, thus dampening the lung inflammation. These results provide insight on the role of ACh in the recovery from ALI. Furthermore, Lipoxygenases (LOXs) are dioxygenases that produce leukotrienes (LTs) from AA. They are nonheme-iron containing dioxygenases. 12(S)-HETE, 15-HETE, and LXs are formed during the metabolism and these metabolites are essential mediators in signal transduction pathways and gene regulation [56]. Leukotrienes play a critical role in inflammation by variety of ways, such as neutrophil recruitment, mucus buildup, smooth muscle constriction, and the development of lung edema. Elevated leukotriene levels due to CS have been evident in several inflammatory disorders and ARDS. Inhibition of their formation could reduce lung inflammation [52,53] and In.Mcx significantly inhibited LOXs. However, further research is required to explore the relation between oxidative stress and inhibition of AChE and LOXs.

Early and sufficient migration of neutrophils and macrophages is crucial for eliminating alveolar debris and harmful substances. CS or oxidative stress impairs their phagocytic potential resulting in severe pulmonary inflammation. Various investigations have been made to attenuate the neutrophilic inflammation in CS-induced lung damage [57]. CS exposure markedlyamplified the cell count, especially neutrophils following CS challenge, in line with previous studies[43,57,58]. Meanwhile, In.Mcx greatly decreased the cell count in a dose-dependent fashion.During ALI/ARDS, pro-inflammatory cytokines and chemokinesare increased in the lungs [43,59]. IL-1β, released by macrophages, may promote cellular differentiation and thereby reinforce the immune activity. However, elevated levels of IL-1β directly affect vascular and epithelial membranes, thus triggering the inflammatory cascade [60]. In.Mcx attenuated cytokines by restricting macrophage and neutrophil infiltration into the lungs, thus, mitigating the damage. The outcomes are consistent with the previous studies where genus *Ipomoea* suppresses inflammatory response by modulating the pro-inflammatory cytokines [61].

CS-induced oxidative stress causes alveolar edema and protein

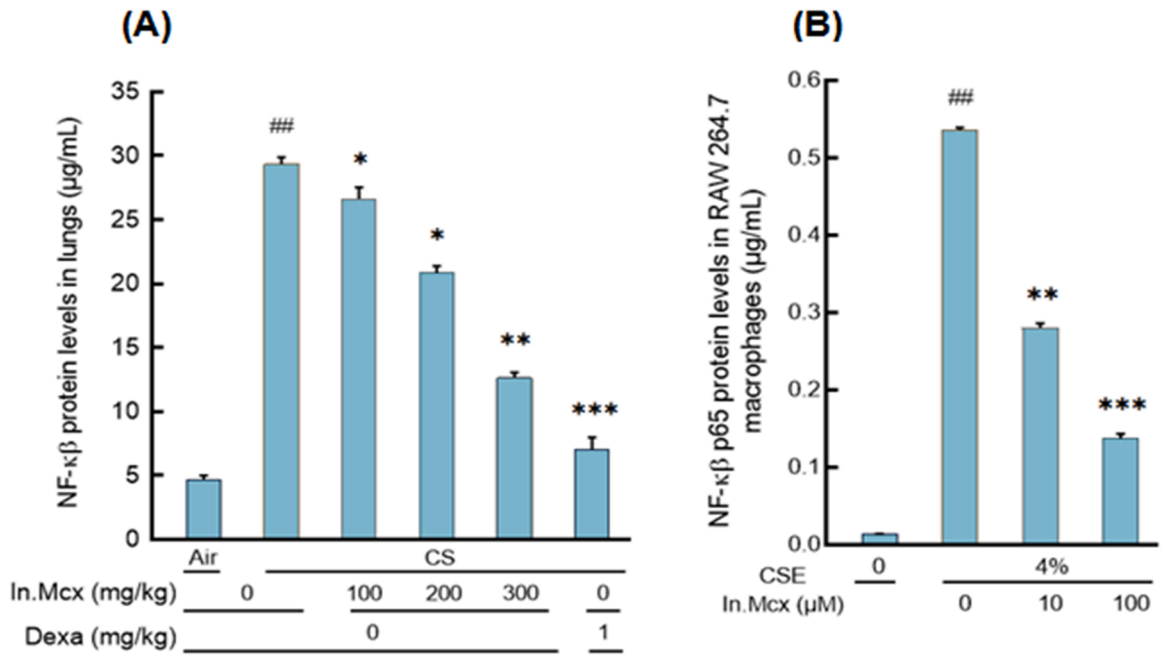

Fig. 11. In.Mcx inhibited the activation of the p65-NF-κB signalling pathway in lungs and RAW 264.7 macrophages in response to CS stimulation. Preserved lung tissues were homogenized and centrifuged at 18,000g for 20 min and the supernatant was collected to measure the expression of p65-NF-κB activation by using the relevant ELISA kit (A). RAW 264.7 macrophages were pretreated with In.Mcx for 1 hr and further treated with CSE (4 %) for 24 hr, and then solubilized cell lysate was collected from the treated RAW 264.7 macrophages for the determination of p65-NF-κB by ELISA (B). $^{\#\#}p < 0.01$ versus control group; $^{**}p < 0.01$, and $^{***}p < 0.001$ as opposed to model group. Findings are communicated as mean ± SEM; n = 3 (each group).

leakage, contributing to hypoxemia. Pulmonary edema increased significantly after CS challenged in CS exposed group [62]. The In. Mcx-treated groups reduced LCW dose-dependently than that of CS-exposed groups. ROS impairs structural integrity to the alveoli, causing significant lung injury. Short-term CS exposure promotes edema, wall thickening, and inflammatory cell invasion, mainly by the neutrophils. Histopathological study and further lung injury score suggested that pre-treatment with In.Mcx reduced the inflammation, alveolar wall damage, and neutrophil intrusion.

Inhalation of CS alters antioxidant activity, resulting in oxidative damage to macromolecules including DNA, lipids and proteins. Oxidative stress may anticipate the advent of inflammation. Thus, oxidative stress markers (namely MDA and MPO) along with ROS, TAC and TOS levels were determined. The uncontrolled neutrophil derived ROS formation, culminating in protein and DNA damage by lipid peroxidation, is considered a key and direct source of oxidative damage to cellular membranes, which are significantly increased in CS exposed group and decreased in In.Mcx pretreated groups. MPO, a proteolytic enzyme, produced by active neutrophils, predicts inflammatory cell adhesion and invasion [63]. MPO activity was greater in CS exposed group [64] while reduced in groups pre-treated with In.Mcx, indicating In.Mcx beneficial effect against pulmonarydamage.The oxidants may trigger lipid peroxidation, resulting in MDA formation (a lipid peroxidation marker) [65]. MDA level was considerably higher in CS-exposed mice, supporting the results of previous studies [66,67]. In.Mcx significantly decreased MDA levels, showing its ability to inhibit lipid peroxidation in CS-induced ALI [68]. The lung defensive system should regulate oxidants with endogenous antioxidants (e.g., molecules, inflammatory cells, and enzymes). Since the study of the discrete antioxidant component is impractical and their antioxidant activity is cumulative, the overall activity of these antioxidants represents the TAC. CS may cause significant reductions in TAC due to the loss of several antioxidant components. TAC increased significantly in In.Mcx, suggesting that In.Mcx may have antioxidant potential. While TOS in CS-exposed mice was significantly high, and this suggests a lack of effectiveness in antioxidative defense systems [57]. However, In.Mcx greatly reduces TOS, confirming its anti-ROS activity. Polyphenol protects in various mechanisms, mostly by downregulating enzymes and sequestering metal cations. According to HPLC analysis, In. Mcx contains a high proportion of polyphenols, and the aforementioned data clearly indicates that In.Mcx potentially acts as a free radical quencher in CS-induced ALI. The in vitro DPPH assay validated In.Mcx's antioxidant activity, as backed by previous studies [26,27].

Following in vivo findings, effects of In.Mcx on RAW 264.7 macrophages using CSE were evaluated in vitro. CSE-activated macrophages have a pathophysiology similar to ALI, making them attractive models for testing anti-inflammatory drugs and finding mediators of pro-inflammatory cytokines and chemokines. In.Mcx (100 μM) considerably decreased cytotoxicity, demonstrating that it may be efficacious in preventing ALI. The ELISA results indicated that CSE-stimulated macrophages produced more IL-6, IL-1β, and KC [69], while these were successfully decreased by In.Mcx treatment, proving the therapy's efficacy.

The transcriptional regulation of various redox-sensitive inflammation-related genes is regulated by NF-κB. Under normal circumstances, NF-κB is usually sequestered in the cytoplasm in inactive form while upon exposure to stimuli like CS or LPS, NF-κB is activated in the nucleus [12]. Elevated NF-κB levels have been reported in CS-exposed ALI murine models [70–72] while targeting NF-κB pathway potentially alleviated lung inflammation by inhibiting pulmonary vascular permeability, reducing pro-inflammatory mediator production, attenuating oxidative stress and improving histopathologic changes [69,70]. Inhibition of NF-κB activation also suppresses the oxidative stress [73]. However, to explore the possible underlying mechanism by which *Ipomoea nil* reduces the oxidative stress and attenuates the generation of pro-inflammatory mediators, effects of *Ipomoea nil* on CS-induced NF-κB activation were studied at both in vivo and in vitro levels. The results revealed that CS-exposure significantly strengthened the IκBα and increased the phosphorylation of NF-κBp65 in the lung tissues and RAW 264.7 macrophages while, as expected and in consistent with previous studies [74–76], the activation of NF-κBp65 signalling was significantly and dose-dependently reduced by *Ipomoea nil* pretreatment. Taken together, *Ipomoea nil* significantly reduced the unchecked inflammatory

response and excessive oxidative stress in the CS-induced ALI by attenuating the activation of the NF-κB pathway.

5. Conclusion

It can be inferred, *Ipomoea nil* has significant potential to inhibit the CS-induced ALI by suppressing the pulmonary infiltration of macrophages and neutrophils, reducing pulmonary edema, attenuating the secretion of proinflammatory chemokines and cytokines in the BALF, alleviating the MPO, MDA, TOS and improving histopathological changes and TEAC expression at both in vitro and in vivo levels. This effect significant may arise through anti-inflammatory and anti-oxidant properties of the *Ipomoea nil* via possibly inhibiting the NF-κB signalling pathway. This means that *Ipomoea nil* has the potential to be employed as a novel pharmacotherapeutic agent for the prevention and treatment of ALI/ARDS. However, future large-scale studies are required to confirm the effects observed and to develop this into a valid therapeutic option.

Funding

No Funding.

CRediT authorship contribution statement

Musaddique Hussain: Conceptualization, Methodology, Formal Analysis, Resources, Project administration. **Ling-Hui Zeng:** Conceptualization, Methodology, Formal Analysis, Resources, Project administration. **Mobeen Fatima:** Writing – original draft, conceptualization. **Saira Shaukat:** Writing – original draft, conceptualization. **Shahzada Khurram Syed:** Writing – original draft, conceptualization. **Ali M. Alqahtani:** Methodology, Project administration, Resources. **Taha Alqahtani:** Methodology, Project administration, Resources. **Amina Mahdy:** Edis Exhibited extensive role during English editing. **Nadia Hussain:** Rephrased and rearranged (reshaped) the manuscript as per recommendation of the respected reviewers. **Muhammad Tariq:** Helped in direct detection of reactive oxygen species. **Abdul Majeed:** Helped in direct detection of reactive oxygen species.

Conflicts of interest statement

The authors declare no conflict of interest.

References

[1] D. Mokrá, Acute lung injury - from pathophysiology to treatment, Physiol. Res 69 (Suppl 3) (2020) p. S353-s366.
[2] M. Hussain, et al., Acute respiratory distress syndrome: bench-to-bedside approaches to improve drug development, Clin. Pharm. Ther. 104 (3) (2018) 484–494.
[3] C.R. Meier, et al., Acute respiratory-tract infections and risk of first-time acute myocardial infarction, Lancet 351 (9114) (1998) 1467–1471.
[4] G. Bellani, et al., Epidemiology, patterns of care, and mortality for patients with acute respiratory distress syndrome in intensive care units in 50 countries, JAMA 315 (8) (2016) 788–800.
[5] M. Merola, B. Blanchard, M.G. Tovey, The kappa B enhancer of the human interleukin-6 promoter is necessary and sufficient to confer an IL-1 beta and TNF-alpha response in transfected human cell lines: requirement for members of the C/EBP family for activity, J. Interferon Cytokine Res 16 (10) (1996) 783–798.
[6] W. MacNee, Oxidants/antioxidants and COPD, Chest 117 (5 Suppl 1) (2000) 303S–317SS.
[7] D. Borgas, et al., Cigarette smoke disrupted lung endothelial barrier integrity and increased susceptibility to acute lung injury via histone deacetylase 6, Am. J. Respir. Cell Mol. Biol. 54 (5) (2016) 683–696.
[8] J.Z. Haeggström, Leukotriene biosynthetic enzymes as therapeutic targets, J. Clin. Investig. 128 (7) (2018) 2680–2690.
[9] M. Rola-Pleszczynski, J. Stanková, Leukotriene B4 enhances interleukin-6 (IL-6) production and IL-6 messenger RNA accumulation in human monocytes in vitro: transcriptional and posttranscriptional mechanisms, Blood 80 (4) (1992) 1004–1011.
[10] M. Sopori, Effects of cigarette smoke on the immune system, Nat. Rev. Immunol. 2 (5) (2002) 372–377.
[11] M. Karin, , Begin. end: IκB kinase (IKK) NF-κB Act. 274 (39) (1999) 27339–27342.
[12] M. Karin, Y.J.Aroi Ben-Neriah, Phosphorylation meets ubiquitination: Control NF-κB Act. 18 (1) (2000) 621–663.
[13] M. Bhatia, S. Moochhala, Role Inflamm. Mediat. Pathophysiol. acute Respir. Distress Syndr. 202 (2) (2004) 145–156.
[14] L.A. Huppert, M.A. Matthay, L.B. Ware, Pathogenesis of acute respiratory distress syndrome. in Seminars in respiratory and critical care medicine, Thieme Medical Publishers, 2019.
[15] M.B. Everhart, et al., Durat. intensity NF-κB Act. determine Sev. Endotoxin-Induc. acute lung Inj. 176 (8) (2006) 4995–5005.
[16] R. Yang, et al., Suppr. NF-κB Pathw. crocetin Contrib. attenuation lipopolysaccharide-Induc. acute lung Inj. mice 674 (2–3) (2012) 391–396.
[17] H. Wu, L. Li, X. Su, Vagus nerve through α7 nAChR modulates lung infection and inflammation: models, cells, and signals, Biomed. Res Int 2014 (2014), 283525.
[18] M. Rosas-Ballina, et al., Acetylcholine-synthesizing T cells relay neural signals in a vagus nerve circuit, Science 334 (6052) (2011) 98–101.
[19] L.V. Borovikova, et al., Vagus nerve stimulation attenuates the systemic inflammatory response to endotoxin, Nature 405 (6785) (2000) 458–462.
[20] S. Kolahian, R. Gosens, Cholinergic regulation of airway inflammation and remodelling, J. Allergy 2012 (2012), 681258.
[21] F.P. Roncon Santana, et al., Nicotinic alpha-7 receptor stimulation (α7nAChR) inhibited NF-kB/STAT3/SOCS3 pathways in a murine model of asthma, Eur. Respir. J. 50 (suppl 61) (2017) OA282.
[22] V.A. Pavlov, et al., Central muscarinic cholinergic regulation of the systemic inflammatory response during endotoxemia, Proc. Natl. Acad. Sci. USA 103 (13) (2006) 5219–5223.
[23] C.P. Khare, Indian Medicinal Plants: An Illustrated Dictionary, Springer, New York, 2008.
[24] M. Hussain, et al., An investigation of the antimicrobial activity of the aqueous, dichloromethane, ethanol and methanol extract of the seeds and whole plant of Ipomoea nil, J. Pharm. Altern. Med. 3 (2014) 14–25.
[25] J.C. Koo, et al., Two hevein homologs isolated from the seed of Pharbitis nil L. exhibit potent antifungal activity, Biochim. Et. Biophys. Acta BBA - Protein Struct. Mol. Enzymol. 1382 (1) (1998) 80–90.
[26] C.L. Lee, et al., New ent-kauran diterpene and antioxidant components from the seed of Ipomoea nil, Nat. Prod. Res (2019) 1–7.
[27] Q. Wang, et al., Optimization of polysaccharides extraction from seeds of Pharbitis nil and its anti-oxidant activity, Carbohydr. Polym. 102 (2014) 460–466.
[28] K.H. Kim, et al., Pharbinilic acid, an allogibberic acid from morning glory (Pharbitis nil), J. Nat. Prod. 76 (7) (2013) 1376–1379.
[29] K.K. Parekh, et al., Antioxidant and cytotoxic activities of few selected Ipomoea species, Pharmacologia 3 (2012) 377–386.
[30] G. Babu, et al., Hepatoprotective activity of ethyl acetate extract of Ipomoea nil (L.) roth seeds on rats, Int. J. Pharm. Pharm. Sci. 5 (2013) 130–133.
[31] M. Zia-Ul-Haq, et al., Compositional study and antioxidant potential of Ipomoea hederacea Jacq. and Lepidium sativum L. Seeds, Molecules 17 (2012) 10306–10321.
[32] H.T. Nguyen, et al., Antibacterial activity of Pharbitin, isolated from the seeds of Pharbitis nil, against various plant pathogenic bacteria, J. Microbiol Biotechnol. 27 (10) (2017) 1763–1772.
[33] S. Ahmad, Anticonvulsant and sex enhancing effects of Ipomoea hederacea seeds extract, Farmacia 62 (2014) 737–742.
[34] K.H. Kim, et al., Identification of antitumor lignans from the seeds of morning glory (Pharbitis nil), J. Agric. Food Chem. 62 (31) (2014) 7746–7752.
[35] J.H. Ju, et al., Induction of apoptotic cell death by Pharbitis nil extract in HER2-overexpressing MCF-7 cells, J. Ethnopharmacol. 133 (1) (2011) 126–131.
[36] Y. Shao, et al., Renal-protective effects of n-hexane layer from morning glory seeds ethanol extract, Biomed. Pharmacother. 95 (2017) 1661–1668.
[37] H.J. Jung, et al., Pharbitis nil (PN) induces apoptosis and autophagy in lung cancer cells and autophagy inhibition enhances PN-induced apoptosis, J. Ethnopharmacol. 208 (2017) 253–263.
[38] M.A. Chaudhry, et al., Ipomoea hederacea Jacq.: a plant with promising antihypertensive and cardio-protective effects, J. Ethnopharmacol. 268 (2021), 113584.
[39] M. Dek, et al., Effects of extraction techniques on phenolic components and antioxidant activity of Mengkudu (Morinda citrifolia L.) leaf extracts, J. Med. Plant Res. 5 (2011).
[40] T. Takao, et al., A Simple screening method for antioxidants and isolation of several antioxidants produced by marine bacteria from fish and shellfish, Biosci., Biotechnol., Biochem. 58 (10) (1994) 1780–1783.
[41] G.L. Ellman, et al., A new and rapid colorimetric determination of acetylcholinesterase activity, Biochem Pharm. 7 (1961) 88–95.
[42] S. Baylac, P. Racine, Inhibition of 5-lipoxygenase by essential oils and other natural fragrant extracts, Int. J. Aromather. 13 (2) (2003) 138–142.
[43] M. Hussain, et al., CRTH2 antagonist, CT133, effectively alleviates cigarette smoke-induced acute lung injury, Life Sci. 216 (2019) 156–167.
[44] L. Van Hoecke, et al., Bronchoalveolar Lavage of Murine Lungs to Analyze Inflammatory Cell Infiltration, J. Vis. Exp.: JoVE 123 (2017) 55398.
[45] J. Feng, et al., Anatomic distribution and morphology of common tracheal/bronchial/pulmonary cells, in: J. Feng, et al. (Eds.), Rapid On-Site Evaluation (ROSE) in Diagnostic Interventional Pulmonology: Volume 1: Infectious Diseases, Springer Singapore, Singapore, 2019, pp. 11–15.
[46] J.C. Parker, M.I. Townsley, Evaluation of lung injury in rats and mice, Am. J. Physiol. Lung Cell. Mol. Physiol. 286 (2) (2004) L231–L246.

[47] M. Hussain, et al., A CRTH2 antagonist, CT-133, suppresses NF-kappaB signalling to relieve lipopolysaccharide-induced acute lung injury, Eur. J. Pharm. 854 (2019) 79–91.
[48] O. Erel, A novel automated direct measurement method for total antioxidant capacity using a new generation, more stable ABTS radical cation, Clin. Biochem 37 (4) (2004) 277–285.
[49] A. Razzaq, et al., Strychnos nux-vomica L. seed Prep. Promot. Funct. Recovery attenuates Oxid. Stress a mouse Model sciatic nerve Crush. Inj. 20 (1) (2020) 1–11.
[50] O. Erel, A new automated colorimetric method for measuring total oxidant status, Clin. Biochem 38 (12) (2005) 1103–1111.
[51] X. Su, et al., Activation of the alpha7 nAChR reduces acid-induced acute lung injury in mice and rats, Am. J. Respir. Cell Mol. Biol. 37 (2) (2007) 186–192.
[52] M. Peters-Golden, W.R. Henderson Jr., Leukotrienes, New Engl. J. Med 357 (18) (2007) 1841–1854.
[53] Y. Ogawa, W.J. Calhoun, The role of leukotrienes in airway inflammation, J. Allergy Clin. Immunol. 118 (4) (2006) 789–798. ; quiz 799-800.
[54] F. Moazed, et al., Cigarette smokers have exaggerated alveolar barrier disruption in response to lipopolysaccharide inhalation, Thorax 71 (12) (2016) 1130.
[55] Y.-Q. He, et al., Natural product derived phytochemicals in managing acute lung injury by multiple mechanisms, Pharmacol. Res. 163 (2021), p. 105224-105224.
[56] R. Mashima, T. Okuyama, The role of lipoxygenases in pathophysiology; new insights and future perspectives, Redox Biol. 6 (2015) 297–310.
[57] Y. Cui, et al., Protective effect of selegiline on cigarette smoke-induced oxidative stress and inflammation in rat lungs in vivo, Ann. Transl. Med. 8 (21) (2020), p. 1418-1418.
[58] W. MacNee, et al., The effect of cigarette smoking on neutrophil kinetics in human lungs, N. Engl. J. Med 321 (14) (1989) 924–928.
[59] J. Pugin, et al., Proinflammatory activity in bronchoalveolar lavage fluids from patients with ARDS, a prominent role for interleukin-1, Am. J. Respir. Crit. Care Med. 153 (6) (1996) 1850–1856.
[60] W. Huvenne, et al., Different regulation of cigarette smoke induced inflammation in upper versus lower airways, Respir. Res. 11 (1) (2010) 100.
[61] M. Majid, et al., Ipomoea batatas L. Lam. ameliorates acute and chronic inflammations by suppressing inflammatory mediators, a comprehensive exploration using in vitro and in vivo models, BMC Complement. Altern. Med. 18 (1) (2018), p. 216-216.
[62] X.Y. Li, et al., Mechanisms of cigarette smoke induced increased airspace permeability, Thorax 51 (5) (1996) 465.
[63] C.C. Winterbourn, A.J. Kettle, M.B. Hampton, Reactive oxygen species and neutrophil function, Annu Rev. Biochem 85 (2016) 765–792.
[64] D. Yu, et al., Isoliquiritigenin Inhibits Cigarette Smoke-Induced COPD by Attenuating Inflammation and Oxidative Stress via the Regulation of the Nrf2 and NF-κB Signaling Pathways, Front. Pharmacol. 9 (2018), p. 1001-1001.
[65] F. Bezerra, et al., Alpha-tocopherol and ascorbic acid supplementation reduced acute lung inflammatory response by cigarette smoke in mouse, Nutrition 22 (11–12) (2006) 1192–1201.
[66] M. Chunhua, et al., Betulin inhibited cigarette smoke-induced COPD in mice, Biomed. Pharm. 85 (2017) 679–686.
[67] M. Dianat, et al., Crocin attenuates cigarette smoke-induced lung injury and cardiac dysfunction by anti-oxidative effects: the role of Nrf2 antioxidant system in preventing oxidative stress, Respir. Res. 19 (1) (2018), p. 58-58.
[68] E.R.N. Herawati, et al., Protective effects of anthocyanin extract from purple sweet potato (Ipomoea batatas l.) on blood mda levels, liver and renal activity, and blood pressure of hyperglycemic rats, Prev. Nutr. Food Sci. 25 (4) (2020) 375–379.
[69] J. Ma, et al., Linalool inhibits cigarette smoke-induced lung inflammation by inhibiting NF-κB activation 29 (2) (2015) 708–713.
[70] J. Yuan, et al., Curcumin attenuates airway inflammation and airway remolding by inhibiting NF-κB signaling and COX-2 in cigarette smoke-induced COPD mice 41 (5) (2018) 1804–1814.
[71] S.-R. Yang, et al., Cigar. smoke induces proinflammatory Cytokine Release Act. NF-κB Post. Modif. histone deacetylase macrophages (2006).
[72] S.K. Manna, et al., Long. Term. Environ. Tob. smoke Act. Nucl. Transcr. Factor-kappa B, Act. Protein-1, Stress responsive kinases mouse brain 71 (11) (2006) 1602–1609.
[73] K.J.Coit Lingappan, NF-κB Oxid. Stress. 7 (2018) 81–86.
[74] N.-R. Shin, et al., Galgeun-tang attenuates Cigar. smoke lipopolysaccharide Induc. Pulm. Inflamm. via IκBα/NF-κB Signal. 23 (10) (2018) 2489.
[75] Q. Liu, et al., Isoliquiritigenin Act. Nucl. Factor erythroid-2 Relat. Factor 2 suppress NOD- Recept. Protein 3 inflammasome Inhib. NF-κB Pathw. macrophages acute lung Inj. 8 (2017) 1518.
[76] N. Ma, et al., Erythromycin Regul. Cigar. smoke-Induc. proinflammatory Mediat. Release Sirtuin 1-Nucl. Factor κB axis macrophages mice lungs 86 (5–6) (2019) 237–247.